Supporting Information for *Size-dependent clustering in phytoplankton communities in a 3D environment* by C. Picoche & F. Barraquand.

S1 Second moment of a point process

In order to familiarize the reader with spatial process metrics, we present here formula for the pair correlation function and Ripley's function for standard point processes (a uniform distribution, i.e. the Poisson point process, and a clustered distribution, the Thomas process), and in the case of the Brownian Bug Model.

S1.1 Pair correlation function

S1.1.1 Standard examples

In the case of a Poisson point process,

$$\forall r \geq 0,\, g_{ii}(r) = 1 \tag{1}$$

For a Thomas point process with parent intensity C_p and child-point position following a normal distribution centered on the parent point with standard deviation σ, the expected value of the pcf is

$$g_{ii}(r) = 1 + \frac{1}{C_p} \frac{1}{(4\pi\sigma^2)^{3/2}} e^{-\left(\frac{r^2}{4\sigma^2}\right)} \tag{2}$$

More generally, for a random superposition stationary point processes with marks (species, in our model) i and j, $\forall i, j, r \geq 0$, $g_{ij}(r) = 1$.

S1.1.2 Brownian Bug Model

We show here how to compute the monospecific pair correlation function using the Brownian Bug Model. In 3 dimensions, when the birth rate λ is the same as the mortality rate μ, the pair density $G(r)$ (where $G(r) = C^2 g(r)$) is a solution of eq. 3 (see Young et al. and Picoche et al. for a detailed explanation).

$$\frac{\partial G}{\partial t} = \frac{2D}{r^2}\frac{\partial}{\partial r}\left(r^2 \frac{\partial G}{\partial r}\right) + \frac{\gamma}{r^2}\frac{\partial}{\partial r}\left(r^4 \frac{\partial G}{\partial r}\right) + 2\lambda C \delta(\boldsymbol{r}) \tag{3}$$

With advection In the presence of advection ($\gamma \neq 0$), a steady-state solution can be found.

$$\begin{aligned}
0 &= \frac{2D}{r^2}\frac{\partial}{\partial r}\left(r^2 \frac{\partial G}{\partial r}\right) + \frac{\gamma}{r^2}\frac{\partial}{\partial r}\left(r^4 \frac{\partial G}{\partial r}\right) + 2\lambda C \delta(\boldsymbol{r}) \\
\Leftrightarrow 0 &= 4\pi r^2 \left(\frac{2D}{r^2}\frac{\partial}{\partial r}\left(r^2 \frac{\partial G}{\partial r}\right) + \frac{\gamma}{r^2}\frac{\partial}{\partial r}\left(r^4 \frac{\partial G}{\partial r}\right) + 2\lambda C \delta(\boldsymbol{r})\right) \\
\Leftrightarrow 0 &= 4\pi \left(2D\frac{\partial}{\partial r}\left(r^2 \frac{\partial G}{\partial r}\right) + \gamma \frac{\partial}{\partial r}\left(r^4 \frac{\partial G}{\partial r}\right)\right) + 4\pi r^2 2\lambda C \delta(\boldsymbol{r})
\end{aligned} \tag{4}$$

We can then integrate Eq. (3) over a small sphere centered on a particle, with radius ρ. Let us first note that

$$\begin{aligned}
\int_{\mathbb{R}^3} \delta(\boldsymbol{r}) d^3\boldsymbol{r} &= 1 \\
\Leftrightarrow \int_0^{2\pi}\int_0^{\pi}\int_0^{\rho} \delta(\boldsymbol{r}') r'^2 \sin(\phi) \; dr' \; d\phi d\theta &= 1 \\
\Leftrightarrow 4\pi \int_0^{\rho} \delta(\boldsymbol{r}') r'^2 dr' &= 1
\end{aligned} \tag{5}$$

Using Eq. (4) and (5),

$$\begin{aligned} 0 &= 4\pi\left(2Dr^2\frac{\partial G}{\partial r}+\gamma r^4\frac{\partial G}{\partial r}\right)+2\lambda C \\ \Leftrightarrow \frac{\partial G}{\partial r} &= -\frac{1}{4\pi}\frac{2\lambda C}{2Dr^2+\gamma r^4} \end{aligned} \tag{6}$$

We can integrate between ρ and ∞, knowing that $G(\infty)=C^2$.

$$C^2-G(\rho) = -\frac{2\lambda C}{4\pi}\int_\rho^\infty \frac{1}{2Dr^2+\gamma r^4}dr \tag{7}$$

We first compute the primitive $A=\int \frac{1}{2Dr^2+\gamma r^4}dr$.

$$\begin{aligned} A &= \int \frac{1}{r^2(2D+\gamma r^2)}dr \\ &= \int \frac{1}{2Dr^2}-\frac{\gamma}{2D(2D+\gamma r^2)}dr \\ &= \frac{1}{2D}\int\frac{1}{r^2}dr-\frac{\gamma}{2D}\int\frac{1}{2D+\gamma r^2}dr \\ &= -\frac{1}{2Dr}-\frac{\gamma}{2D}\int\frac{1}{2D\left(1+\left(\sqrt{\frac{\gamma}{2D}}r\right)^2\right)} \end{aligned} \tag{8}$$

With a change of variable $u=\sqrt{\frac{\gamma}{2D}}r$, using $\int\frac{1}{1+u^2}=\arctan(u)$, we have:

$$A=-\frac{1}{2Dr}-\frac{\sqrt{\gamma}\arctan\left(\frac{\sqrt{\gamma}r}{\sqrt{2D}}\right)}{2\sqrt{2}D\sqrt{D}}+K \tag{9}$$

where K is a constant.
We can know compute $B=[A]_\rho^\infty$.

$$B=-\frac{\sqrt{\gamma}\pi}{4\sqrt{2}D\sqrt{D}}+\frac{1}{2D\rho}+\frac{\sqrt{\gamma}\arctan\left(\frac{\sqrt{\gamma}\rho}{\sqrt{2D}}\right)}{2\sqrt{2}D\sqrt{D}} \tag{10}$$

This leads to:

$$\begin{aligned} G(\rho) &= C^2+\frac{2\lambda C}{4\pi}B \\ &= C^2+\frac{\lambda C}{2\pi}\left[\frac{1}{2D\rho}+\frac{\sqrt{\gamma}\arctan\left(\frac{\sqrt{\gamma}\rho}{\sqrt{2D}}\right)}{2\sqrt{2}D\sqrt{D}}-\frac{\sqrt{\gamma}\pi}{4\sqrt{2}D\sqrt{D}}\right] \end{aligned} \tag{11}$$

Finally, the pair correlation function $g=G/C^2$ is defined as

$$g(\rho)=\frac{\lambda}{4\pi CD}\left(\frac{\sqrt{\gamma}\arctan\left(\frac{\sqrt{\gamma}\rho}{\sqrt{2D}}\right)}{\sqrt{2D}}+\frac{1}{\rho}-\frac{\pi\sqrt{\gamma}}{2\sqrt{2D}}\right)+1 \tag{12}$$

Without advection When $U=0$, $\gamma=0$ and there is no steady solution. We can get back to Eq. (3).

$$\frac{\partial G}{\partial t}=\frac{2D}{r^2}\frac{\partial}{\partial r}\left(r^2\frac{\partial G}{\partial r}\right)+2\lambda C\delta(\boldsymbol{r}) \tag{13}$$

Assuming an isotropic environment, this means

$$\frac{\partial G}{\partial t}-2D\Delta G=2\lambda C\delta(\boldsymbol{r}) \tag{14}$$

where $\Delta=\nabla^2$ is the Laplacian operator.
We therefore have

$$\mathcal{L}G(\boldsymbol{r},t)=2\lambda C\delta(\boldsymbol{r}) \tag{15}$$

where $\mathcal{L}$ is the linear differential operator $\partial_t-2D\Delta$.

Using the Green's function theory, we know that $G(y)=\int H(y,s)2\lambda C\delta(s)ds$ where $H(y,s)=H(y-s)$ is the Green kernel (heat kernel).

$$
\begin{aligned}
G(\boldsymbol{r},t) &= 2\lambda C \int_{\mathbb{R}^3}\int_0^t H(\boldsymbol{r}-\boldsymbol{r'},t')\delta(\boldsymbol{r'})dr'dt' \\
\Leftrightarrow \quad &= 2\lambda C \int_0^t H(\boldsymbol{r},t')dt'
\end{aligned}
$$

A solution for the Green's function using $\mathcal{L} = \partial_t - 2D\Delta$ in 3 dimensions is $H(r,t) = \left(\frac{1}{4\pi 2Dt}\right)^{3/2}\exp(\frac{-r^2}{4\times 2Dt})$. $G(r,t)$ can then be computed:

.

$$
G(r,t) = 2\lambda C\left(\frac{erf\left(\frac{r}{\sqrt{8tD}}\right)}{8\pi Dr} + K\right) \tag{16}
$$

where erf is the error function. Using $G(r,0) = C^2$ and $\lim_{x\to+\infty} erf = 1$ in Eq. (16),

$$
\begin{array}{ccc}
C^2 & = & 2\lambda C\left(\frac{1}{8\pi Dr} + K\right) \\
\Leftrightarrow \frac{C}{2\lambda} + & \frac{1}{8\pi Dr} = & K
\end{array} \tag{17}
$$

We can finally compute G(r,t):

$$
\begin{aligned}
G(r,t) &= 2\lambda C\left(\frac{erf\left(\frac{r}{\sqrt{8tD}}\right)}{8\pi Dr} + \frac{C}{2\lambda} + \frac{1}{8D\pi r}\right) \\
&= \frac{\lambda C}{4\pi Dr}\left\{1 - erf\left(\frac{r}{\sqrt{8Dt}}\right)\right\} + C^2 \\
\Leftrightarrow g(r,t) &= \frac{\lambda}{4D\pi rC}\left\{1 - erf\left(\frac{r}{\sqrt{8Dt}}\right)\right\} + 1
\end{aligned} \tag{18}
$$

S1.2 Ripley's K-function

S1.2.1 Standard examples

In the case of a Poisson point process,

$$
\forall r \geq 0,\ K_{ii}(r) = \frac{4}{3}\pi r^3 \tag{19}
$$

For a Thomas point process,

$$
K_{ii}(r) = \frac{4}{3}\pi r^3 + \frac{1}{\lambda_p \sigma\sqrt{\pi}}\left(\sigma\sqrt{\pi}erf\left(\frac{r}{2\sigma}\right) - re^{-\left(\frac{r}{2\sigma}\right)^2}\right) \tag{20}
$$

More generally, for a random superposition of stationary point processes, $K_{ij}(r) = \frac{4}{3}\pi r^3$.

S1.2.2 Brownian Bug Model

We can integrate the pcf formula to compute Ripley's K-function, as $g(r) = \frac{K'(r)}{4\pi r^2}$.

With advection From eq. 12,

$$
K(\rho) = 4\pi\int_0^\rho r^2 + \frac{\lambda}{2\pi C}\left[\frac{r}{2D} + \frac{\sqrt{\gamma}r^2\arctan\left(\frac{\sqrt{\gamma}r}{\sqrt{2D}}\right)}{2\sqrt{2}D\sqrt{D}} - \frac{\sqrt{\gamma}\pi r^2}{4\sqrt{2}D\sqrt{D}}\right]dr \tag{21}
$$

We define $A = \int_0^\rho r^2 dr$, $B = \int_0^\rho \frac{r}{2D}dr$, $C = \int_0^\rho r^2\arctan\left(\frac{\sqrt{\gamma}r}{\sqrt{2D}}\right)dr$ and $E = \int_0^\rho \frac{\sqrt{\gamma}\pi r^2}{4\sqrt{2}D\sqrt{D}}dr$.

$$
\begin{array}{ll}
A = & \frac{1}{3}\rho^3 \\
B = & \frac{\rho^2}{4D} \\
E = & \frac{\sqrt{\gamma}\pi\rho^3}{12\sqrt{2}D\sqrt{D}}
\end{array} \tag{22}
$$

We can also compute $C = \int_0^\rho r^2\arctan\left(\frac{\sqrt{\gamma}r}{\sqrt{2D}}\right)dr$. We can first change variable, with $u = \frac{r}{\sqrt{2D}}$,$dr = \sqrt{2D}du$.

$$\begin{aligned} C &= \int_0^{\rho/\sqrt{2D}} (\sqrt{2D}u)^2 \arctan(\sqrt{\gamma}u)\sqrt{2D}du \\ &= (2D)^{3/2} \int_0^{\rho/\sqrt{2D}} u^2 \arctan(\sqrt{\gamma}u)du \end{aligned} \tag{23}$$

We can integrate by parts, with $f = \arctan(\sqrt{\gamma}u)$ and $g' = u^2$.

$$\begin{aligned} C &= (2D)^{3/2} \left(\frac{\rho^3}{3(2D)^{3/2}} \arctan(\sqrt{\frac{\gamma}{2D}}\rho) - \int_0^{\rho/\sqrt{2D}} \frac{\sqrt{\gamma}u^3}{3(\gamma u^2+1)}du \right) \\ &= (2D)^{3/2} \left(\frac{\rho^3}{3(2D)^{3/2}} \arctan(\sqrt{\frac{\gamma}{2D}}\rho) - \frac{\sqrt{\gamma}}{3} \int_0^{\rho/\sqrt{2D}} \frac{u^3}{(\gamma u^2+1)}du \right) \end{aligned} \tag{24}$$

We can substitute $v = \gamma u^2 + 1$,$du = \frac{1}{2\gamma u}dv$.

$$\begin{aligned} \int_0^{\rho/\sqrt{2D}} \frac{u^3}{(\gamma u^2+1)}du &= \frac{1}{2\gamma^2} \int_1^{\gamma\rho^2/2D+1} \frac{v-1}{v}dv \\ &= \frac{1}{2\gamma^2} \int_1^{\gamma\rho^2/2D+1} 1 - \frac{1}{v}dv \\ &= \frac{1}{2\gamma^2}(\gamma\frac{\rho^2}{2D} - \log(\gamma\frac{\rho^2}{2D}+1)) \end{aligned} \tag{25}$$

Going back to C, we obtain:

$$\begin{aligned} C &= \frac{\rho^3 \arctan(\sqrt{\frac{\gamma}{2D}}\rho)}{3} - (2D)^{3/2} \frac{\sqrt{\gamma}}{3} \frac{1}{2\gamma^2} \left(\frac{\gamma}{2D}\rho^2 - \log(\gamma\frac{\rho^2}{2D}+1) \right) \\ &= \frac{\rho^3 \arctan(\sqrt{\frac{\gamma}{2D}}\rho)}{3} - \frac{\sqrt{2D}}{6\sqrt{\gamma}}\rho^2 + \frac{\sqrt{2}D^{3/2}}{3\gamma^{3/2}} \log(\gamma\frac{\rho^2}{2D}+1) \end{aligned} \tag{26}$$

Combining all equations:

$$\begin{aligned} K(\rho) &= \frac{4}{3}\pi\rho^3 + \frac{2\lambda}{C} \left(\frac{\rho^2}{4D} + \frac{\sqrt{\gamma}\rho^3 \arctan(\sqrt{\frac{\gamma}{2D}}\rho)}{6\sqrt{2}D^{3/2}} - \frac{\rho^2}{12D} + \frac{\log\left(\gamma\frac{\rho^2}{2D}+1\right)}{6\gamma} - \frac{\sqrt{\gamma}\pi\rho^3}{12\sqrt{2}D\sqrt{D}} \right) \\ &= \frac{4}{3}\pi\rho^3 + \frac{2\lambda}{C} \left(\frac{\rho^2}{6D} + \frac{\sqrt{\gamma}\rho^3 \arctan(\sqrt{\frac{\gamma}{2D}}\rho)}{6\sqrt{2}D^{3/2}} + \frac{\log\left(\gamma\frac{\rho^2}{2D}+1\right)}{6\gamma} - \frac{\sqrt{\gamma}\pi\rho^3}{12\sqrt{2}D\sqrt{D}} \right) \end{aligned} \tag{27}$$

Without advection From eq. 18,

$$\begin{aligned} K(\rho) &= \frac{\lambda}{DC} \int_0^\rho r \left\{ 1 - erf\left(\frac{r}{\sqrt{8Dt}}\right) \right\} + 4\pi r^2 dr \\ &= \frac{\lambda}{CD} \left(\frac{\rho^2}{2} - \int_0^\rho r \times erf\left(\frac{r}{\sqrt{8Dt}}\right) dr \right) + \frac{4}{3}\pi\rho^3 \end{aligned} \tag{28}$$

We first compute the primitive for $\int_0^\rho r \times erf\left(\frac{r}{\sqrt{8Dt}}\right) dr$. We define $u = \frac{r}{\sqrt{8Dt}}$, $dr = \sqrt{8Dt}du$.

$$\int_0^\rho r \times erf\left(\frac{r}{\sqrt{8Dt}}\right) dr = 8Dt \int_0^{\rho/\sqrt{8Dt}} u \times erf\,(u)\, du \tag{29}$$

We can integrate by parts, with $f = erf(u)$ and $g' = u$.

$$8Dt \int_0^{\rho/\sqrt{8Dt}} u \times erf\,(u)\, du = 8Dt \left(\frac{\rho^2}{2}\frac{1}{8Dt} erf(\frac{\rho}{\sqrt{8Dt}}) - \frac{1}{\sqrt{\pi}} \int_0^{\rho/\sqrt{8Dt}} u^2 e^{-u^2} du \right) \tag{30}$$

We integrate by parts again, this time with $f = u$ and $g' = ue^{-u^2}$, which leads to

$$\int u^2 e^{-u^2} du = -\frac{ue^{-u^2}}{2} + \frac{1}{2}\int e^{-u^2} du = -\frac{ue^{-u^2}}{2} + \frac{\sqrt{\pi}erf(u)}{4} \tag{31}$$

If we use eq. 31 in eq. 30:

$$\begin{aligned} 8Dt \int_0^{\rho/\sqrt{8Dt}} u \times erf\,(u)\, du &= 8Dt \left(\frac{\rho^2}{2}\frac{1}{8Dt} erf(\frac{\rho}{\sqrt{8Dt}}) - \frac{erf(\frac{\rho}{\sqrt{8Dt}})}{4} + \frac{1}{2\sqrt{\pi}}\frac{\rho}{\sqrt{8Dt}} e^{-\rho^2/8Dt} \right) \\ \Leftrightarrow \int_0^\rho r \times erf\left(\frac{r}{\sqrt{8Dt}}\right) dr &= \frac{1}{2} erf(\frac{\rho}{\sqrt{8Dt}})(\rho^2 - 4Dt) + \frac{\sqrt{2Dt}}{\sqrt{\pi}}\rho e^{-\rho^2/8Dt} \end{aligned} \tag{32}$$

We can now compute $K(\rho)$.

$$K(\rho) = \frac{\lambda}{CD} \left(\frac{\rho^2}{2} - \frac{1}{2} erf(\frac{\rho}{\sqrt{8Dt}})(\rho^2 - 4Dt) - \frac{\sqrt{2Dt}\rho}{\sqrt{\pi}} e^{-\rho^2/8Dt} \right) + \frac{4}{3}\pi\rho^3 \tag{33}$$

S2 Dominance index

In this section, we define the dominance index, give its theoretical formula for several point processes, and compare them to our own simulations.

S2.1 Definition

The dominance index (defined in Table S1 in the Supporting Information of Wiegand *et al.*, 2007) is the ratio between conspecifics and all individuals surrounding a given particle. Formally, the dominance $D_i(r)$ of species i for radius r can be written:

$$D_i(r) = \frac{C_i K_{ii}(r)}{\sum_{j=1}^{S} C_j K_{ij}(r)} \tag{34}$$

where C_i is the concentration of species i.

In the following, we assume we study a random superposition of point processes, i.e. $K_{ij}(r) = \frac{4}{3}\pi r^3$

S2.2 Classical point processes

In the Poisson point process, $K_{ii}(r) = K_{ij}(r)$, which means the dominance index can be reduced to ratios of concentrations:

$$D_i(r) = \frac{C_i}{\sum_{j=1}^{S} C_j} \tag{35}$$

In the Thomas process, using eq. 20,

$$D_i(r) = \frac{C_i \left(\frac{4}{3}\pi r^3 + \frac{F(r)}{\lambda_{p,i}}\right)}{C_i \frac{F(r)}{\lambda_{p,i}} + \sum_j C_j \frac{4}{3}\pi r^3} \tag{36}$$

with $F(r) = \frac{1}{\sigma\sqrt{\pi}}\left(\sigma\sqrt{\pi} erf\left(\frac{r}{2\sigma}\right) - re^{-\left(\frac{r}{2\sigma}\right)^2}\right)$.

S2.3 Brownian Bug Model

Based on the formula for Ripley's function for the BBM , in the presence of advection, the dominance index follows eq. 37.

$$D_i(r,t) = \frac{C_i \left[\frac{4}{3}\pi r^3 + \frac{\lambda}{3C_i D}\left(r^2 + \frac{\sqrt{\gamma} r^3 \arctan(\sqrt{\frac{\gamma}{2D}} r)}{\sqrt{2D}} + \frac{D\log\left(\gamma\frac{r^2}{2D}+1\right)}{\gamma} - \frac{\sqrt{\gamma}\pi r^3}{2\sqrt{2D}}\right)\right]}{\sum_{j=1}^{S} C_j \frac{4}{3}\pi r^3 + \frac{\lambda}{3D}\left(r^2 + \frac{\sqrt{\gamma} r^3 \arctan(\sqrt{\frac{\gamma}{2D}} r)}{\sqrt{2D}} + \frac{D\log\left(\gamma\frac{r^2}{2D}+1\right)}{\gamma} - \frac{\sqrt{\gamma}\pi r^3}{2\sqrt{2D}}\right)} \tag{37}$$

In the absence of advection,

$$D_i(r,t) = \frac{C_i \left[\frac{4}{3}\pi r^3 + \frac{\lambda}{C_i D}\left(\frac{r^2}{2} - \frac{1}{2} erf(\frac{r}{\sqrt{8Dt}})(r^2 - 4Dt) - \frac{\sqrt{2Dt} r}{\sqrt{\pi}} e^{-r^2/8Dt}\right)\right]}{\sum_{j=1}^{S} C_j \frac{4}{3}\pi r^3 + \frac{\lambda}{D}\left(\frac{r^2}{2} - \frac{1}{2} erf(\frac{r}{\sqrt{8Dt}})(r^2 - 4Dt) - \frac{\sqrt{2Dt} r}{\sqrt{\pi}} e^{-r^2/8Dt}\right)} \tag{38}$$

S3 Computation of the pair correlation function and Ripley's function

The algorithm for pcf computation was mostly taken from the function `pcf3est` in spatstat 2.2-0 (Baddeley *et al.*, 2015) and adapted to interspecific pcf.

Schematically, $g(r)$ is estimated via the use of the Epanechnikov kernel κ_E with bandwidth δ.

$$\hat{g}(r) \quad = \quad \frac{1}{C^2}\frac{1}{4\pi r^2}\sum_i \sum_j \kappa_E(r - ||x_i - x_j||) w(x_i, x_j) \tag{39}$$

where $w(x_i, x_j)$ is the Ohser translation correction estimator (Ohser, 1983-01-01) and the kernel is defined as follow.

$$\kappa_E(x) = \begin{cases} \frac{3}{4\delta}\left(1 - \frac{x^2}{\delta^2}\right) & \text{for } -\delta \leq x \leq \delta \\ 0 & \text{otherwise} \end{cases} \tag{40}$$

The estimate $\hat{g}(r)$ is therefore very sensitive to the bandwidth: if it is too small, the estimate is noisy and may even be missing several pairs of points; if it is too large, the smoothing might be so important that values are strongly underestimated. In spatstat 2.2-0 (Baddeley *et al.*, 2015), the bandwidth default value is $\delta = 0.26C^{-1/3}$. The pcf computation function was first tested on standard distributions (with the default bandwidth), then on the Brownian Bug Model (with different bandwidths, see below).

Estimates of the Ripley's function were also performed with the Ohser translation correction estimator but did not require any kernel smoothing.

S3.1 Standard point processes

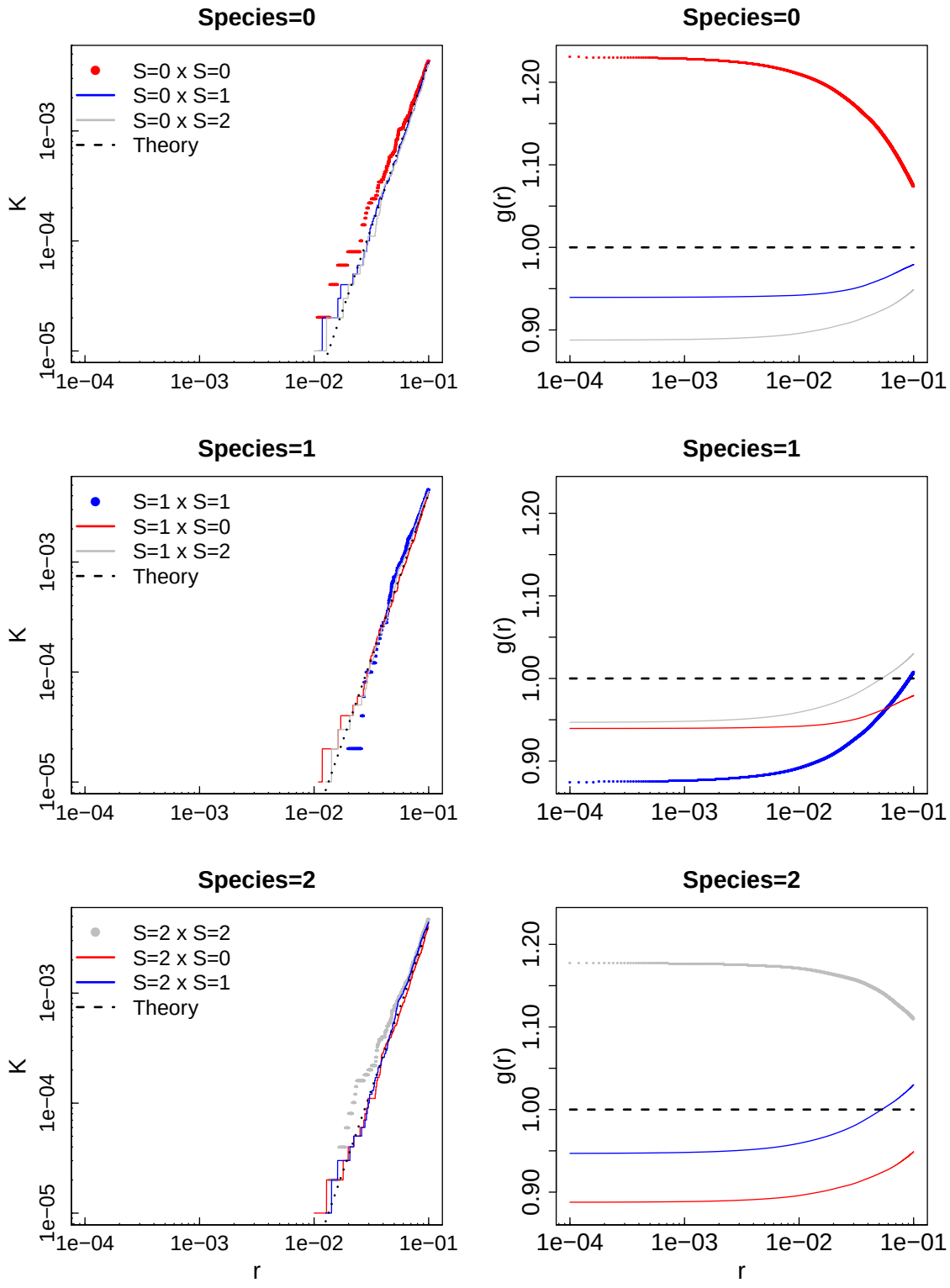

Figure S1: Intra- and inter-specific Ripley's K function and PCF values for 3 species following a Poisson process with intensity 10 cm^{-3}, in a volume of 1000 cm^3. Values computed from our simulations (circles and solid lines for intra- and interspecific values, respectively) are compared with theoretical formula (dotted lines). Note that theoretical values are the same for intra and interspecific moments for the Poisson distribution. Colors correspond to the different species (red for species 0, blue for species 1, black for species 2).

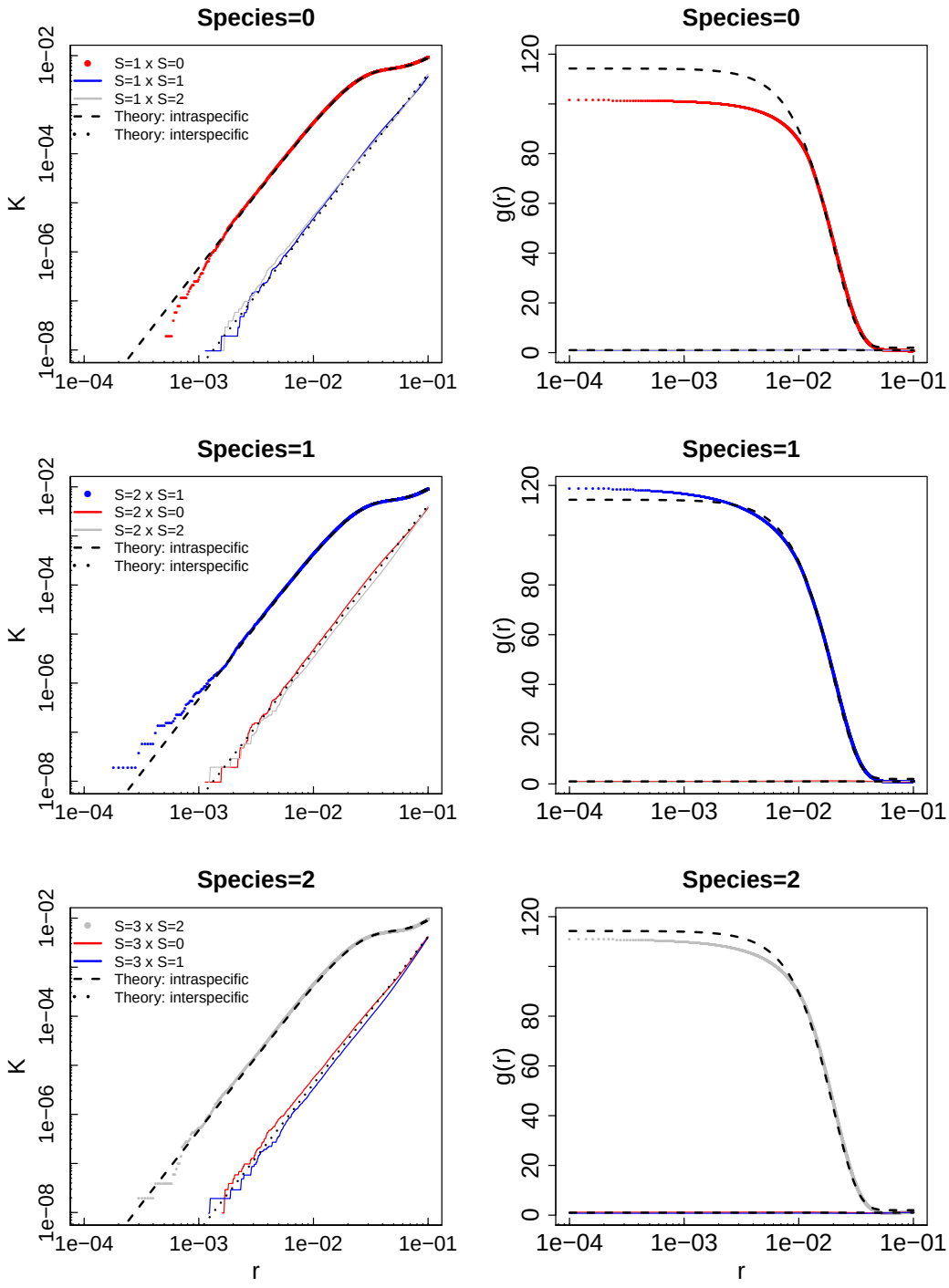

Figure S2: Intra- and inter-specific Ripley's K function and PCF values for 3 species following a Thomas process with parent intensity $\lambda_p = 200$ cm^{-3}, number of children per parent $N_c = 50$, in a volume of 1 cm^3, $\sigma = 0.01$ and $\delta \approx 0.012$. Values computed from our simulations (circles and solid lines for intra- and interspecific values, respectively) are compared with theoretical formula (dashed and dotted lines for intra- and interspecific values, respectively). Colors correspond to the different species (red for species 0, blue for species 1, black for species 2).

S3.2 Brownian Bug Model

While the pcf was one of the first indices we intended to use, we quickly realized that the combination of the large range of radii we wanted to explore (from 10^{-4} to 1 cm) and the low density of particles, at least for microphytoplankton, made the estimation difficult as the choice of the bandwidth was critical. We give an example

of the sensitivity of the pcf computation to the bandwidth below (Fig. S3).

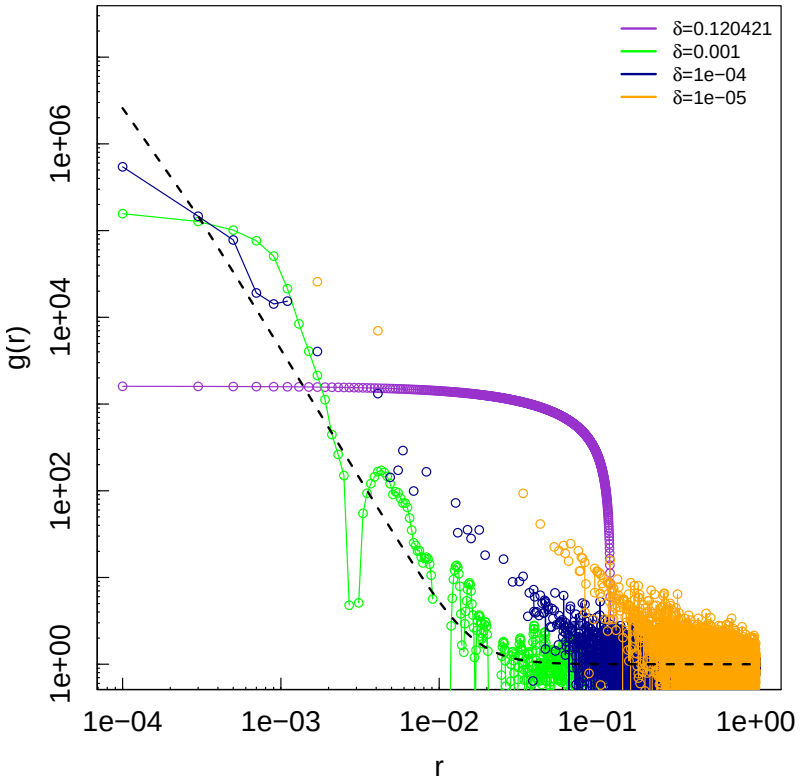

Figure S3: Intraspecific pcf computed for the Brownian bug model with microphytoplankton particles, after 1000 time steps, with different values of the bandwidth δ. The dashed line indicates the theoretical pcf.

We decided, from these results, to focus on Ripley's function, which enabled us to compute the dominance index without having to calibrate a bandwidth beforehand.

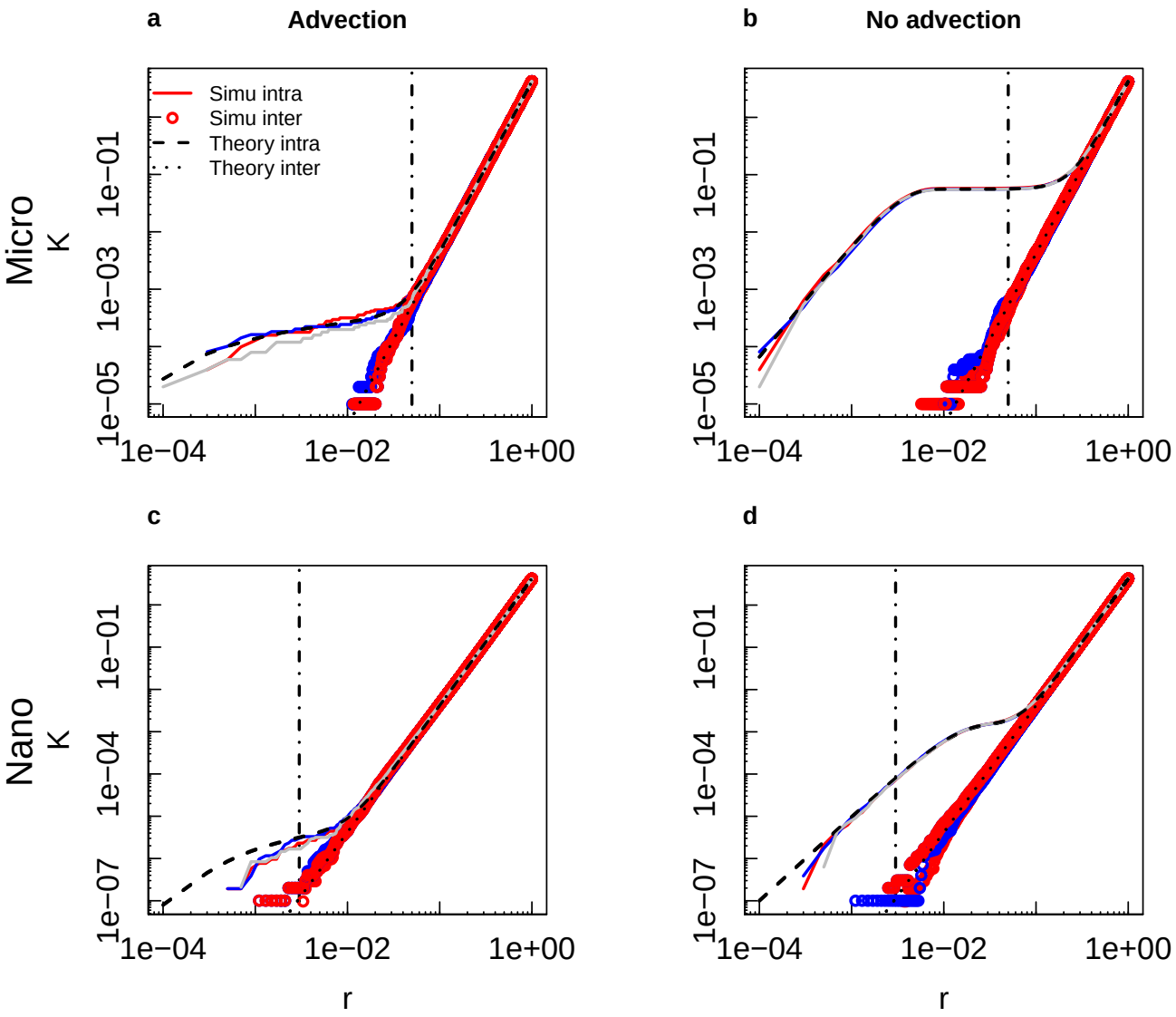

Figure S4: Ripley's K function for microphytoplankton (a-b) and nanophytoplankton (b-c) in a 3-species community with even distributions after 1000 timesteps, with (a, c) and without (b, d) advection. Each color represents a different species. The black dashed line corresponds to the 10-diameter threshold considered as the maximum range for nutrient-based competition.

References

Baddeley, A., Rubak, E. & Turner, R. (2015). *Spatial Point Patterns: Methodology and Applications with R*. Chapman and Hall/CRC Press, London.

Ohser, J. (1983-01-01). On estimators for the reduced second moment measure of point processes. *Series Statistics*, 14, 63–71.

Wiegand, T., Gunatilleke, C.V.S., Gunatilleke, I.A.U.N. & Huth, A. (2007). How individual species structure diversity in tropical forests. *Proceedings of the National Academy of Sciences*, 104, 19029–19033.